

Magnetic Response in Mesoscopic Rings and Moebius Strips: A Theoretical Study

Santanu K. Maiti^{†,‡,1}

[†]*Theoretical Condensed Matter Physics Division, Saha Institute of Nuclear Physics,
1/AF, Bidhannagar, Kolkata-700 064, India*

[‡]*Department of Physics, Narasinha Dutt College, 129 Belilious Road, Howrah-711 101, India*

Abstract

We investigate magnetic response in mesoscopic rings and moebius strips penetrated by magnetic flux ϕ . Based on a simple tight-binding framework all the calculations are performed numerically which describe persistent current and low-field magnetic susceptibility as functions of magnetic flux ϕ , total number of electrons N_e , system size N and disorder strength W . Our exact analysis may provide some important signatures to study magnetic response in nano-scale loop geometries.

PACS No.: 73.22.-f; 73.23.-b; 73.23.Ra; 75.20.-g

Keywords: Mesoscopic ring; Moebius strip; Persistent current; Low-field magnetic susceptibility; Disorder.

¹**Corresponding Author:** Santanu K. Maiti
Electronic mail: santanu.maiti@saha.ac.in

1 Introduction

More advanced nanoscience and technology has made it possible to fabricate devices whose dimensions are comparable to mean free path of an electron and electron transport in such systems gives several novel and interesting new phenomena. In the mesoscopic regime, phase coherence of the electronic states are of fundamental importance, and the phenomenon of persistent current is a spectacular consequence of quantum phase coherence in this regime. Experimental investigations on these systems have provided several surprising quantum behaviors in contrast to those anticipated from the classical theory of metals. At much low temperatures, two aspects of the new quantum regime appear that are of particular interest.

(i) The phase coherence length L_ϕ , the length scale over which an electron maintains its phase memory, increases significantly with the decrease of temperature and is comparable to the system size L .

(ii) The energy levels of these small finite size systems are discrete.

These two are the essential criteria for the existence of persistent current in these systems upon the application of an external magnetic flux ϕ . Many theoretical works [1, 2, 3, 4, 5, 6, 7, 8, 9, 10, 11, 12, 13, 14, 15, 16, 17, 18] on persistent current in one-dimensional (1D) mesoscopic rings are available in literature, yet they cannot clearly explain several results those have been obtained experimentally. The discovery of persistent current in mesoscopic rings has addressed new interesting questions on the thermodynamics of these systems. Although such an effect was predicted several years ago, the unexpectedly large amplitudes of measured currents lead to many important questions. It has been proposed that the electron-electron (e-e) interactions contribute significantly to the average currents. Although, an explanation based on the perturbative calculation both in interaction and disorder, seems to give a quantitative estimate closer to the experimental results but still it is less than the mea-

sured currents by an order of magnitude, and the interaction parameter used in the theory is not well understood physically. Though the enhancement of current amplitude can be understood by some theoretical arguments [16, 17, 18] but the sign of the currents cannot be predicted precisely. Levy *et al.* [19] have observed diamagnetic response for the measured currents at low fields in the experiment on 10^7 isolated mesoscopic Cu rings. While, Chandrasekhar *et al.* [20] have measured ϕ_0 periodic currents in Ag rings with paramagnetic response near zero fields. In a theoretical work Cheung *et al.* [4] have predicted that the direction of current is random depending on the total number of electrons in the system and the specific realization of the random potentials. On the other hand, Yu and Fowler [12] have shown both diamagnetic and paramagnetic responses in mesoscopic Hubbard rings. In an experiment, Jariwala *et al.* [21] have obtained diamagnetic persistent currents with both h/e and $h/2e$ flux periodicities in an array of 30-diffusive gold rings. Similar diamagnetic sign of the currents in the vicinity of zero magnetic field were also found in an experiment [22] on 10^5 disconnected Ag rings. Thus we can emphasize that the prediction of the sign of low-field currents is a major challenge in this area. It has been studied that only for single-channel rings, the sign of the low-field currents can be mentioned exactly [23, 24]. While, in all other cases i.e., for multi-channel rings and cylinders, sign of the low-field currents cannot be predicted exactly. Hence we see that the sign of low-field currents is not very clear and the theoretical and experimental results still do not agree very well. Therefore, we can say that the phenomenon of persistent current in metallic systems gives an exciting curiosity and is an open subject.

The paper is organized as follows. Following the brief introduction (Section 1), in Section 2, we describe the behavior of persistent current in strictly one-channel mesoscopic rings. The effect of intrachain interaction on persistent current in moebius strips is discussed in Section 3. Section 4 illus-

trates the behavior of low-field magnetic susceptibility both for one-channel mesoscopic rings and moebius strips, and finally, we summarize our study in Section 5.

2 Persistent current in one-channel mesoscopic rings

Here we explore the behavior of persistent current in strictly one-channel mesoscopic rings. Let us start by referring to Fig. 1 where a mesoscopic ring is penetrated by a magnetic flux ϕ . To describe the

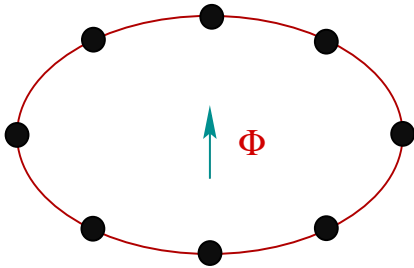


Figure 1: Schematic view of a 1D mesoscopic ring penetrated by a magnetic flux ϕ . The filled black circles correspond to the position of atomic sites. A persistent current I is established in the ring.

system we use a tight-binding framework. Within a non-interacting electron picture, the tight-binding Hamiltonian for a N -site ring, enclosing a magnetic flux ϕ (in units of the elementary flux quantum $\phi_0 = ch/e$), can be expressed in Wannier basis as,

$$H = \sum_i \epsilon_i c_i^\dagger c_i + \sum_{\langle ij \rangle} v \left(e^{i\theta} c_i^\dagger c_j + e^{-i\theta} c_j^\dagger c_i \right) \quad (1)$$

where, ϵ_i 's are the on-site energies, v is the hopping strength between nearest-neighbor atomic sites and $\theta = 2\pi\phi/N$ is the phase factor due to the flux threaded by the ring. As the magnetic field associated with flux ϕ does not penetrate anywhere of the circumference of the ring, we neglect Zeeman term in the above Hamiltonian (Eq. 1). Throughout our calculations we set the hopping strength $v = -1$ and use the units where $c = e = h = 1$.

In order to study current-flux (I - ϕ) characteristics first it is necessary to know the variation of energy levels with ϕ . For an ordered ring, we calculate the energy eigenvalues analytically. Mathematically, the energy eigenvalue for n -th eigenstate can be written in the form,

$$E_n(\phi) = 2v \cos \left[\frac{2\pi}{N} \left(n + \frac{\phi}{\phi_0} \right) \right] \quad (2)$$

where, n is an integer bounded in the range $-N/2 \leq n < N/2$. But as long as impurities are introduced in the ring i.e., the ring becomes a disordered one, energy eigenvalues cannot be obtained analytically. In that case we do exact numerical diagonalization of the tight-binding Hamiltonian to achieve the eigenvalues. As illustrative examples, in Fig. 2

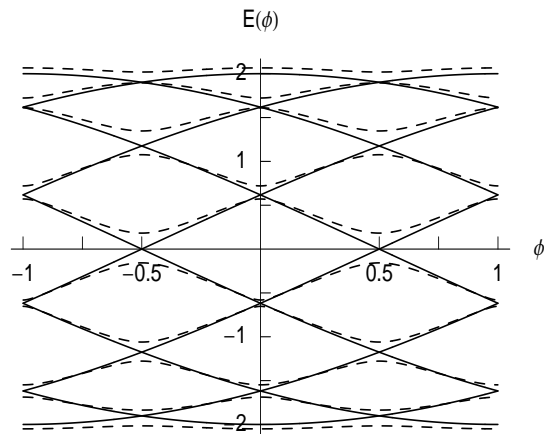


Figure 2: Energy-flux characteristics for ordered (solid line) and disordered (dotted line) mesoscopic rings with $N = 10$. For the disordered case, we choose $W = 1$.

we plot the energy-flux (E - ϕ) characteristics for a mesoscopic ring considering $N = 10$. The solid and dotted curves correspond to the perfect and disordered rings, respectively. For the disordered ring, we set $W = 1$. In absence of any impurity ($W = 0$), energy levels intersect with each other at integer or half-integer multiples of $\phi_0/2$, while gaps open at these points in presence of impurity. In both the two cases energy levels vary periodically as a function of ϕ showing ϕ_0 ($= 1$, in our chosen unit

$c = e = h = 1$) flux-quantum periodicity.

The current I_n carried by n -th energy level having energy E_n is obtained by taking the 1-st order derivative of E_n with flux ϕ . Mathematically it can be expressed as,

$$I_n = -\frac{\partial E_n}{\partial \phi} \quad (3)$$

At absolute zero temperature ($T = 0\text{K}$), total current of a system, described with fixed number of electrons N_e , will be obtained by taking the sum of

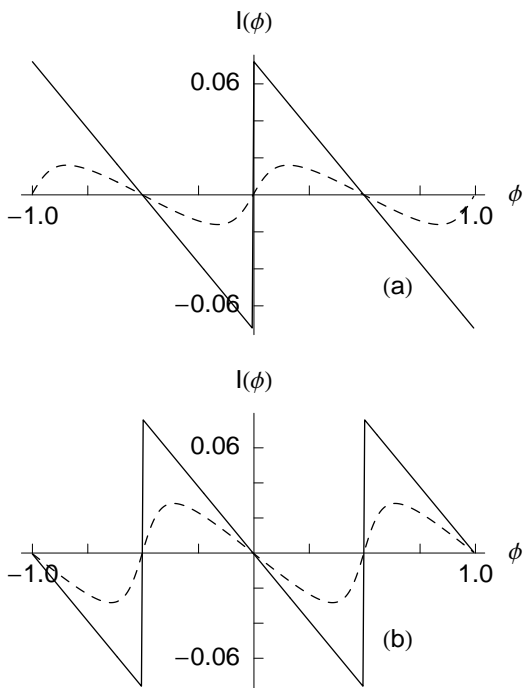


Figure 3: Persistent current as a function of ϕ for ordered (solid line) and disordered (dotted line) mesoscopic rings with $N = 150$, where (a) $N_e = 50$ and (b) $N_e = 55$. For the disordered case, we fix $W = 1$.

individual contributions from the lowest N_e energy levels. Thus, we can write the total current in the form,

$$I(\phi) = \sum_n I_n(\phi) \quad (4)$$

As representative examples, in Fig. 3 we show the variation of persistent current for a typical mesoscopic ring considering $N = 150$, where (a) and (b) represent the results for even ($N_e = 50$) and odd

($N_e = 55$) number of electrons, respectively. The solid and dotted curves correspond to the perfect ($W = 0$) and disordered ($W = 1$) rings, respectively. For the ordered ring, we set $\epsilon_i = 0$ for all i , while for the disordered case site energies (ϵ_i) are chosen randomly from a ‘‘Box’’ distribution function of width $W = 1$. From the results it is observed that, in impurity free rings current exhibits saw-tooth like variation as a function of ϕ providing sharp transitions, associated with the crossing of energy levels, at $\phi = \pm n\phi_0$ or $\pm n\phi_0/2$, depending on whether the ring contains even or odd number of electrons. On the other hand, this saw-tooth like behavior completely disappears as long as impurities are introduced in the ring. This is due to the fact that, in presence of impurities all the degeneracies move out, and accordingly, energy levels vary continuously with ϕ which provide continuous variation of the current. Addition to this feature, it is also important to note that in disordered ring current amplitude gets reduced significantly compared to the ordered one. Such a behavior can be well understood from the theory of Anderson localization, where we get more localization with the increase of disorder strength W [25]. Both for perfect and dirty rings, persistent current varies periodically with ϕ showing only ϕ_0 flux-quantum periodicity.

3 Persistent current in moebius strips

This section describes the behavior of persistent current in moebius strips. Persistent current in a moebius strip is highly sensitive on the intra-chain interaction strength and here we will focus our study in this particular aspect. The schematic view of a moebius strip, penetrated by a magnetic flux ϕ , is shown in Fig. 4. The vertical line connecting the atomic sites in upper and lower strands is called as ‘rung’. In presence of magnetic flux ϕ , the tight-binding Hamiltonian for a moebius strip with N rungs (i.e., $2N$ atomic sites since in each strand

there are N atomic sites) can be written within the non-interacting electron picture as,

$$H = \sum_{i=1}^{2N} \epsilon_i c_i^\dagger c_i + v \sum_{i=1}^{2N} \left(e^{i\theta} c_i^\dagger c_{i+1} + e^{-i\theta} c_{i+1}^\dagger c_i \right) + v_\perp \sum_{i=1}^{2N} c_i^\dagger c_{i+N} \quad (5)$$

where, ϵ_i represents the on-site energy of an electron in site i and $\theta = 2\pi\phi/N$ is the phase factor associated with flux ϕ . v gives the nearest-neighbor hopping integral in each strand and v_\perp corresponds to the hopping strength between the nearest-neighbor sites in the two strands, the so-called intra-chain interaction strength. It (v_\perp) significantly controls the periodicity of persistent current in such a spe-

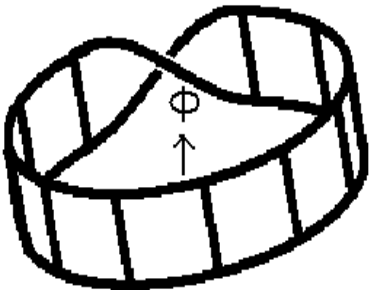


Figure 4: Schematic representation of a moebius strip penetrated by a magnetic flux ϕ .

cial type of geometric model which we will describe in forthcoming sub-section.

Now we start our discussion with the energy-flux characteristics of a moebius strip. For illustrative examples, in Fig. 5 we plot the energy levels as a function of ϕ for a moebius strip considering $N = 5$ in the typical case where $v_\perp = 0$. The solid and dotted lines correspond to the perfect and disordered moebius strips, respectively. The presence (disordered strip) or absence (ordered strip) of W provides exactly the similar behavior i.e., gap or gap less spectrum as we observe in the case of one-channel mesoscopic rings. Most importantly we notice that the energy levels have extremas at integer multiples of $\phi = \pm n\phi_0/4$ or $\pm n\phi_0/2$. Addition

to this, it is also observed that the energy levels vary periodically with flux ϕ providing $\phi_0/2$ flux-

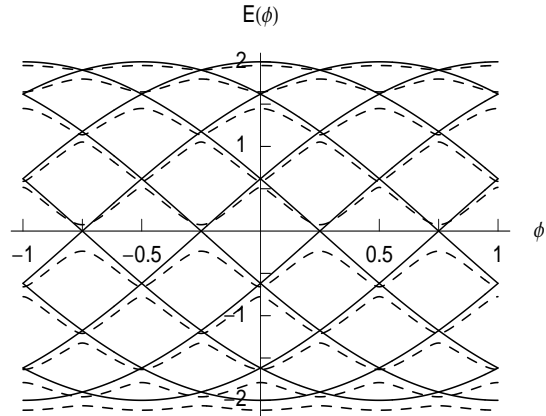


Figure 5: Energy-flux characteristics for ordered (solid curve) and disordered (dotted curve) moebius strips ($N = 5$) with $v_\perp = 0$.

quantum periodicity instead of simple ϕ_0 periodicity, as observed in traditional one-channel mesoscopic rings or multi-channel cylinders. This phenomenon of half flux-quantum periodicity can be explained as follow. In the typical case where

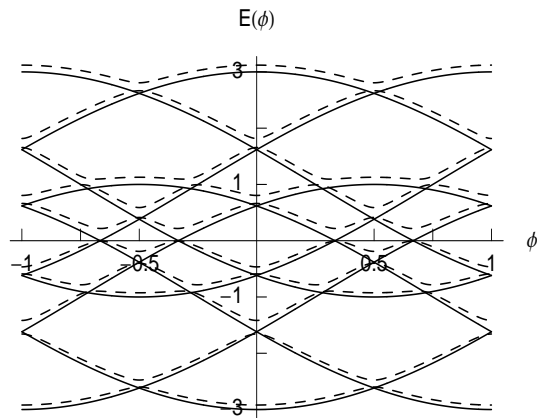


Figure 6: Energy-flux characteristics for ordered (solid line) and disordered (dotted line) moebius strips ($N = 5$) with $v_\perp = -1$.

$v_\perp = 0$, electrons cannot able to hop along the vertical direction. Therefore, in a moebius strip if an electron starts to move from any point, it will come back at its initial position after traversing twice the path length, and accordingly, it encloses 2ϕ flux.

This provides $\phi_0/2$ flux-quantum periodicity and it is the speciality of such a twisted geometry. Now, as long as electrons are allowed to hop between the two strands i.e., $v_\perp \neq 0$, energy levels get back ϕ_0 flux-quantum periodicity. This is quite obvious since for the case when $v_\perp \neq 0$ one can treat the moebius strip as a conventional cylinder. For illustrations,

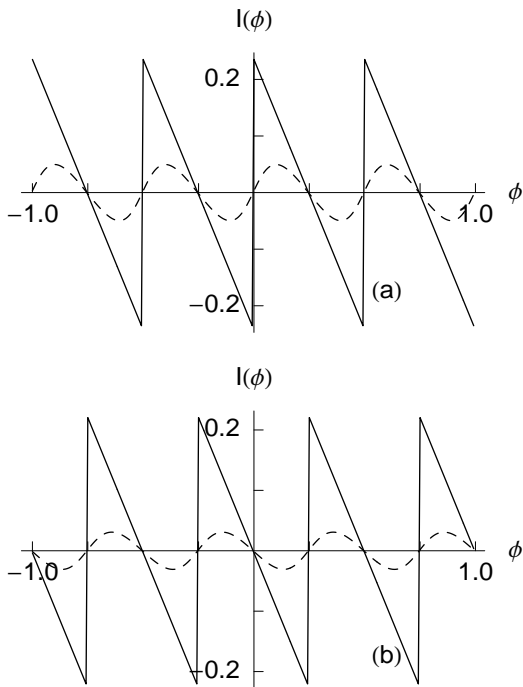


Figure 7: I - ϕ characteristics for ordered (solid curve) and disordered (dotted curve) moebius strips ($N = 50$) with $v_\perp = 0$. (a) $N_e = 40$ and (b) $N_e = 35$. For the disordered case, $W = 1$.

see the results plotted in Fig. 6, where the solid and dotted lines correspond to the identical meaning as in Fig. 5.

With the above energy-flux characteristics now we concentrate our study on the current-flux spectra. Let us begin with the results plotted in Fig. 7, where the currents are evaluated for some moebius strips with $v_\perp = 0$. The system size N is fixed at 50, where (a) and (b) correspond to $N_e = 40$ (even) and 35 (odd), respectively. The solid and dotted curves represent the currents for ordered and disordered moebius strips, respectively, where the disor-

der strength W is set to 1. Like single channel mesoscopic ring, persistent current reveals saw-tooth like behavior as a function of ϕ both for odd and even number of electrons. Similarly, in presence of disorder current varies continuously, as studied earlier,

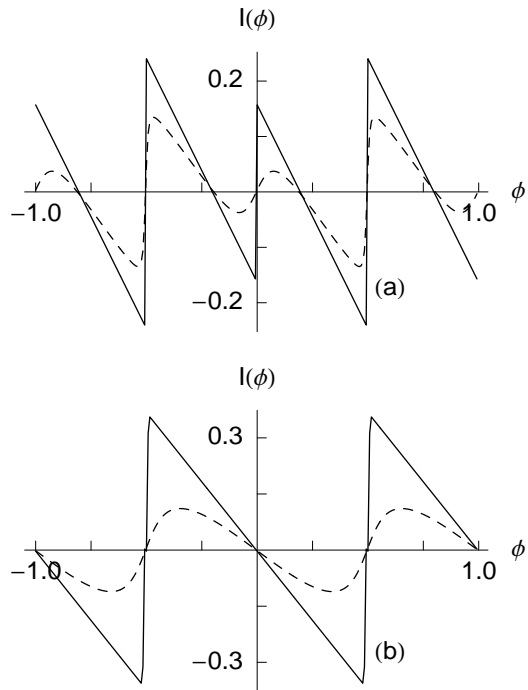


Figure 8: I - ϕ characteristics for ordered (solid curve) and disordered (dotted curve) moebius strips ($N = 50$) with $v_\perp = -1$. (a) $N_e = 40$ and (b) $N_e = 35$. For the disordered case, W is fixed at 1.

and gets much reduced value than the perfect case. These features are clearly understood from our previous discussion. The main point is that, for this particular case where $v_\perp = 0$, current varies periodically with ϕ showing $\phi_0/2$ periodicity, instead of conventional ϕ_0 periodicity. This unconventional period halving behavior of persistent current may be clearly visible from our energy-flux spectrum, for instance see Fig. 5.

The situation becomes quite different when electrons can able to hop along the transverse direction i.e., for $v_\perp \neq 0$. In this case a moebius can be regarded as an ordinary mesoscopic cylinder, and therefore, we get the conventional features of persis-

tent current. For illustrative purposes, in Fig. 8 we show the current-flux characteristics for some typical moebius strips ($N = 50$) considering $v_{\perp} = -1$, where (a) and (b) correspond to the results for $N_e = 40$ and 35, respectively. The solid and dotted lines represent the similar meaning as in Fig. 7. The saw-tooth like behavior is still preserved in perfect case. But, some additional kinks may appear in I - ϕ spectrum at different values of ϕ depending on the choices of N_e . For instance, the current shows a kink across $\phi = 0$ when $N_e = 40$. These kinks are associated with the crossing of energy levels for the cylindrical systems. While, for disordered cases, current varies continuously with much reduced amplitude, as expected, and no kink will appear.

4 Low-field magnetic susceptibility

Next, we focus our attention on the determination of magnetic susceptibility $\chi(\phi)$ in the limit $\phi \rightarrow 0$. Evaluating the sign of $\chi(\phi)$ one can able to predict whether the current is paramagnetic or diamagnetic in nature. It was a long standing problem over the past few many years, and, here we try to emphasize about it both for one-channel rings and moebius strips described with fixed number of electrons N_e . The general expression of magnetic susceptibility at any flux ϕ is expressed in the form,

$$\chi(\phi) = \frac{N^3}{16\pi^2} \left(\frac{\partial I(\phi)}{\partial \phi} \right) \quad (6)$$

where, N corresponds to the total number of atomic sites in the system. Here we will determine $\chi(\phi)$ only in the limit $\phi \rightarrow 0$ i.e., we are interested only on the low-field magnetic susceptibility.

As representative examples, in Fig. 9 we display the variation of low-field magnetic susceptibility as a function of N_e for strictly one-channel mesoscopic rings, where (a) and (b) correspond to the perfect ($W = 0$) and disordered ($W = 1$) rings, respectively. The system size N is fixed at 200. Our re-

sults predict that in absence of any impurity $\chi(\phi)$ is always negative irrespective of the total number of electrons N_e i.e., whether N_e is odd or even. It reveals that for perfect rings low-field current provides only the diamagnetic response. This diamagnetic behavior of low-field currents can be clearly understood by noting the slope of I - ϕ characteristics plot-

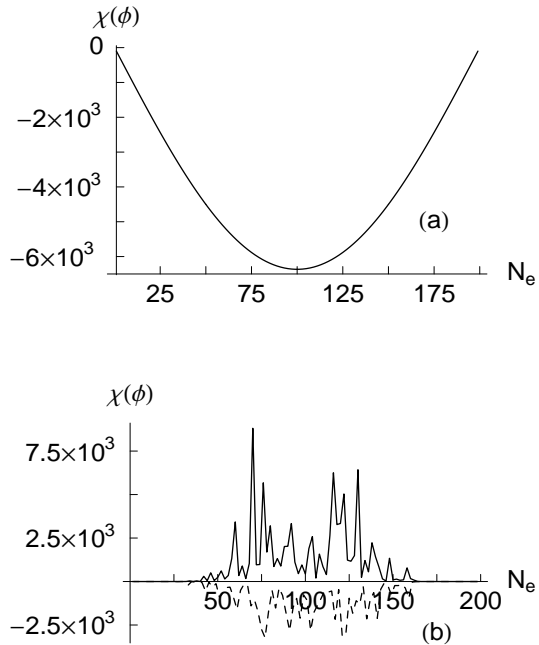


Figure 9: Low-field magnetic susceptibility $\chi(\phi)$ as a function of N_e for (a) ordered rings and (b) disordered ($W = 1$) rings considering $N = 200$. The solid and dotted curves in (b) correspond to the results for even and odd N_e , respectively.

ted by the solid lines in Figs. 3(a) and (b). The response drastically changes as long as impurities are introduced in the system (9(b)). For odd and even N_e , it shows completely opposite behavior. The low-field current gives paramagnetic response for the rings with even N_e (solid line), while for the rings with odd N_e it shows diamagnetic nature (dotted line). These diamagnetic and paramagnetic natures of persistent current for the disordered case can be easily understood by observing the slopes of I - ϕ curves presented by the dotted

lines in Figs. 3(a) and (b). All these features are equally valid irrespective of disorder strength and disordered configurations. Thus, in brief we can say that for one-channel rings described with fixed number of electrons, sign of low-field currents can be precisely determined.

At the end, we focus on the behavior of low-field magnetic response in moebius geometries. For these systems, sign of low-field currents strongly depends on the strength of intra-chain interaction (v_{\perp}). For $v_{\perp} = 0$, a moebius strip becomes a single channel ring, and therefore, sign of low-field currents can be mentioned exactly according to the above prescription. On the other hand for the case where v_{\perp} is finite, sign of low-field currents cannot be predicted accurately as it strongly depends on the number of electrons and specific realization of disordered configuration in the strips.

5 Concluding remarks

To summarize, we have studied the behavior of persistent current and low-field magnetic susceptibility in strictly one-channel mesoscopic rings and moebius strips penetrated by magnetic flux ϕ . A tight-binding framework is given to describe the system, where all calculations are done numerically to study the magnetic response. In perfect rings current shows saw-tooth like variation as a function of ϕ , while it varies continuously in disordered rings. Both for perfect and disordered rings current varies periodically with ϕ exhibiting ϕ_0 flux-quantum periodicity. In moebius strips a unconventional $\phi_0/2$ periodic nature of persistent current is observed for the particular case when $v_{bot} = 0$. While, current gets back its ϕ_0 periodicity when electrons are able to hop along the transverse direction i.e., $v_{\perp} \neq 0$. In the study of low-field magnetic response we have seen that for one-channel mesoscopic rings described with constant number of electrons, sign of low-field currents can be mentioned precisely. While, for moebius strips with $v_{\perp} \neq 0$,

sign of low-field currents cannot be predicted exactly as it depends on the number of electrons as well as disordered configurations. Our exact analysis can provide some physical insight to study magnetic response in mesoscopic loop geometries.

References

- [1] N. Byers and C. N. Yang, Phys. Rev. Lett. **7**, 46 (1961).
- [2] M. Büttiker, Y. Imry, and R. Landauer, Phys. Lett. **96A**, 365 (1983).
- [3] H. F. Cheung, Y. Gefen, E. K. Riedel, and W. H. Shih, Phys. Rev. B **37**, 6050 (1988).
- [4] H. F. Cheung and E. K. Riedel, Phys. Rev. Lett. **62**, 587 (1989).
- [5] G. Montambaux, H. Bouchiat, D. Sigeti, and R. Friesner, Phys. Rev. B **42**, 7647 (1990).
- [6] B. L. Altshuler, Y. Gefen, and Y. Imry, Phys. Rev. Lett. **66**, 88 (1991).
- [7] F. von Oppen and E. K. Riedel, Phys. Rev. Lett. **66**, 84 (1991).
- [8] A. Schmid, Phys. Rev. Lett. **66**, 80 (1991).
- [9] V. Ambegaokar and U. Eckern, Phys. Rev. Lett. **65**, 381 (1990).
- [10] G. Bouzerar, D. Poilblanc, and G. Montambaux, Phys. Rev. B **49**, 8258 (1994).
- [11] T. Giamarchi and B. S. Shastry, Phys. Rev. B **51**, 10915 (1995).
- [12] N. Yu and M. Fowler, Phys. Rev. B **45**, 11795 (1992).
- [13] I. O. Kulik, Physica B **284**, 1880 (2000).
- [14] K. Yakubo, Y. Avishai, and D. Cohen, Phys. Rev. B **67**, 125319 (2003).

- [15] E. H. M. Ferreira, M. C. Nemes, M. D. Sampaio, and H. A. Weidenmüller, *Phys. Lett. A* **333**, 146 (2004).
- [16] S. K. Maiti, *Int. J. Mod. Phys. B* **21**, 179 (2007).
- [17] S. K. Maiti, J. Chowdhury, and S. N. Karmakar, *Synthetic Metals* **155**, 430 (2005).
- [18] S. K. Maiti, J. Chowdhury, and S. N. Karmakar, *J. Phys.: Condens. Matter* **18**, 5349 (2006).
- [19] L. P. Levy, G. Dolan, J. Dunsmuir, and H. Bouchiat, *Phys. Rev. Lett.* **64**, 2074 (1990).
- [20] V. Chandrasekhar, R. A. Webb, M. J. Brady, M. B. Ketchen, W. J. Gallagher, and A. Kleinsasser, *Phys. Rev. Lett.* **67**, 3578 (1991).
- [21] E. M. Q. Jariwala, P. Mohanty, M. B. Ketchen, and R. A. Webb, *Phys. Rev. Lett.* **86**, 1594 (2001).
- [22] R. Deblock, R. Bel, B. Reulet, H. Bouchiat, and D. Mailly, *Phys. Rev. Lett.* **89**, 206803 (2002).
- [23] S. K. Maiti, *Phy. Scr.* **73**, 519 (2006); [Addendum: *Phy. Scr.* **78**, 019801 (2008)].
- [24] S. K. Maiti, *Physica E* **31**, 117 (2006).
- [25] P. A. Lee and T. V. Ramakrishnan, *Rev. Mod. Phys.* **57**, 287 (1985).